THE EUROPEAN SOCIETY OF MEDICINE
Medical Research Archives, Volume 14 Issue 1

RESEARCH ARTICLE

Polyoxometalates-mediated regulation of melanin biosynthesis and macrophage function in skin homeostasis

Katsuyuki Fujinami*[1,2], Nanami Tominaga[1], Katsuaki Dan[3,4], Toshiko Tanaka-Kagawa[2], Ikuo Kawamura[2]

[1]FSX Inc., 1-12-3, Izumi, Kunitachi, Tokyo 186-0012, Japan
[2]Department of Health Medicine, Yokohama University of Pharmacy, 601, Matano-cho, Totsuka-ku, Yokohama 245-0066, Japan
[3]Division of Research and Development, Research Organization of Biological Activity, Ebisu-nishi 5F, 2-8-4, Ebisu-nishi, Shibuya-ku, Tokyo 150-0021, Japan
[4]Department of Pathophysiology, Yokohama University of Pharmacy, 601, Matano-cho, Totsuka-ku, Yokohama 245-0066, Japan

OPEN ACCESS

PUBLISHED
31 January 2025

CITATION
Fujinami, et al., 2025. Polyoxometalates-mediated regulation of melanin biosynthesis and macrophage function in skin homeostasis. Medical Research Archives, [online] 14(1).

ISSN
2375-1924

ABSTRACT

The skin is a complex multilayered organ that performs essential functions such as barrier protection, immune and chemical defense, sensory perception, and metabolic regulation. Physiological homeostasis can be influenced by psychosocial stress, aging, and immune cell activity in the tissue microenvironment. Among resident cells, fibroblasts synthesize extracellular matrix components, while melanocytes generate melanin, the pigment responsible for freckles and age spots.

Cutaneous homeostasis is continuously maintained through immune surveillance. Macrophages play a crucial role by phagocytosing foreign materials and senescent cells, as well as producing nitric oxide, cytokines, and chemokines that regulate inflammation. Recent studies have suggested that skin macrophages recognize aged cells via stabilin-1 (STAB1), remove them through phagocytosis, and release fibroblast growth factor-2 (FGF2) to signal neighboring stem cells, thus promoting regeneration. Polyoxometalates (PMs) exhibit a remarkable diversity of structural motifs, comprising clusters formed through hydrogen bonding between basic units. These basic units are composed of transition metal atoms coordinated by six or eight oxygen atoms. These compounds exhibit antibacterial and antiviral properties, and have attracted attention for their potential use in dermatological and anti-aging applications. Three PMs—VB1 ($VOSO_4$), VB2 ($K_{11}H[(VO)_3(SbW_9O_{33})_2]\cdot 27H_2O$), and VB3 ($Na_2[SbW_9O_{34}]\cdot 19H_2O$)—have been reported to demonstrate antioxidant and anti-aging effects in skin fibroblasts and mesenchymal stem cells, mediated in part by enhanced cystine uptake and, possibly, the subsequent enhancement of glutathione synthesis. In this study, we employed a three-dimensional human epidermal model comprising keratinocytes and melanocytes to demonstrate that VBs influence melanin synthesis and penetrate the epidermal layer. The potential effects of VBs on macrophage-mediated regulation of senescence and tissue regeneration were also investigated using the human monocytic U937 cell line. Taken together, these results indicate that VBs inhibit melanin synthesis by suppressing tyrosinase activity. Furthermore, VBs can penetrate the epidermal layer and act on macrophages localized in the dermis, where they upregulate STAB1 and FGF2 expression. These findings suggest that VBs modulate macrophage functions through enhanced recognition of senescent cells and regenerative signaling. Indeed, VBs were experimentally confirmed to upregulate STAB1 and FGF2 expression in macrophages using the U937 cell line. It is likely that they act as bioactive compounds that modulate pigment metabolism and immune homeostasis, as well as contribute to skin renewal and anti-aging-related processes.

Introduction

Dermatology has potential applications in regenerative medicine and anti-aging research.[1-4] The skin serves as a protective barrier, contributing to immune and chemical defense, sensory perception, and metabolic regulation. Stress and emotions can also affect skin disorders.[5]

The skin has a three-layered structure consisting of the epidermis, dermis, and subcutaneous tissue. Various cells exist in each layer and perform diverse roles.[6] Fibroblasts secrete many components that build the extracellular matrix.[7] Melanin, which causes spots and freckles, is produced by melanocytes. The generated melanin is transferred to keratinocytes due to aging or skin issues. Melanin lingers in the skin for extended periods due to factors such as delayed keratinocyte turnover, leading to the formation of spots.[8-9] Melanogenesis begins with the oxidation of L-tyrosine to L-DOPA, catalyzed by tyrosinase, and then to dopaquinone. The pathway proceeds to yellow pheomelanin in the presence of cysteine or to black eumelanin when cysteine is absent.[10] Both are collectively referred to as melanin.

Immune cells constantly monitor the skin tissue to defend against external invasion and maintain skin homeostasis. Macrophages play a crucial role by phagocytosing foreign bodies and senescent cells.[11] Activated macrophages produce nitric oxide, tumor necrosis factor alpha (TNF-α), several cytokines, and chemokines, which play a central role in inflammatory responses.[12] In recent years, a mechanism has been proposed in which skin macrophages recognize aged skin cells via stabilin-1 (STAB1), eliminate them through phagocytosis, and then signal nearby skin stem cells to regenerate skin cells by secreting fibroblast growth factor-2 (FGF2), thereby indicating that elimination has occurred.[13]

Polyoxometalates (PMs) possess diverse structures that include clusters are formed through hydrogen bonding between basic units. These units are composed of transition metal atoms coordinated by six or eight oxygen atoms.[14] The biological activities related to the anti-aging effects of PMs with proven antibacterial and antiviral activity (VB1: $VOSO_4$, VB2: $K_{11}H[(VO)_3(SbW_9O_{33})_2]\cdot 27H_2O$, and VB3: $Na_2[SbW_9O_{34}]\cdot 19H_2O$) are being researched. Although these are currently used in products such as hand towels and hand soap, their cosmetic formulations are being developed to allow use not only for hand hygiene but also for whole-body care.[15]

The mechanism of action of VBs on skin cells is being investigated. Treatment with VBs enhance the expression of advanced glycation end-product (AGE) receptors that protect cells against glycation stress and suppress the accumulation of reactive oxygen species (ROS) induced by oxidative (H_2O_2) stress.[16] This effect appears stronger in VB2 and VB1. However, VB3 is thought to promote stress resistance by stimulating mesenchymal stem cells (MSCs) and inducing functional changes in exosomes secreted by these cells. One proposed mechanism involves increased cystine uptake, which in turn promotes the synthesis of glutathione, an intracellular antioxidant.[17]

Previous studies have primarily used cultured fibroblasts, but a three-dimensional (3D) skin model was used here to investigate responses more closely resembling those observed *in vivo*. The 3D human skin model (MEL-300-B) uses an epidermal model containing keratinocytes and melanocytes. This facilitates continuous application of test samples to the epidermis and can be maintained in culture for approximately 3 w by periodically replacing the culture medium in the lower chamber.[18] During the experiment, it is possible to acquire images of the skin surface (changes in color tone over time). After completing the experiment, tissue can be collected to prepare pathological specimens or to extract proteins and nucleic acids from the tissue, allowing measurement of melanin content, tyrosinase activity, and levels of various mRNAs.[19] By collecting the culture medium from the lower chamber and detecting the elements contained in VBs (VB1: V, S; VB2, VB3: W, Sb), the transmittance rate to the dermis can also be determined. Using this experimental system, the

objectives of this study were to verify the effects of VB1, VB2, and VB3 on melanin synthesis in a skin model, to examine their rate of penetration into the dermis, and to investigate the effects of VBs on macrophages that contribute to maintaining skin homeostasis.

Materials and Methods

POLYOXOMETALATES

Vanadyl sulfate (VB1) was purchased from Fujifilm Wako Pure Chemical Industries Ltd. (Osaka, Japan). Bulk powders of VB2: $K_{11}H[(VO)_3(SbW_9O_{33})_2]\cdot 27H_2O$ and VB3: $Na_2[SbW_9O_{34}]\cdot 19H_2O$ were synthesized using a patented method (International Patent Publication Number: WO2019/230210). Each bulk powder was ground in a mortar, dissolved in ultrapure water, and the solution was filtered through a 0.45-µm filter before use in the experiment.[17] The VB concentration was set at 100 µg/mL, as this level showed no cytotoxic effects and maintained stable efficacy throughout the experiments.

HUMAN SKIN 3D MODEL

The skin model (MEL-300-B; PermeGear Inc., Riegelsville, PA, USA) was purchased from Clabow Co. (Osaka, Japan). After a 1-d preculture in the dedicated medium (EPI-100-NMM-113) at 37°C in 5% CO_2 and 95% humidified air, experiments were initiated. Cultures were maintained for 22 d, with medium replacement and reagent application every other day. Each well of the 12-well plate contained one skin tissue insert placed in a chamber (Fig. 1).

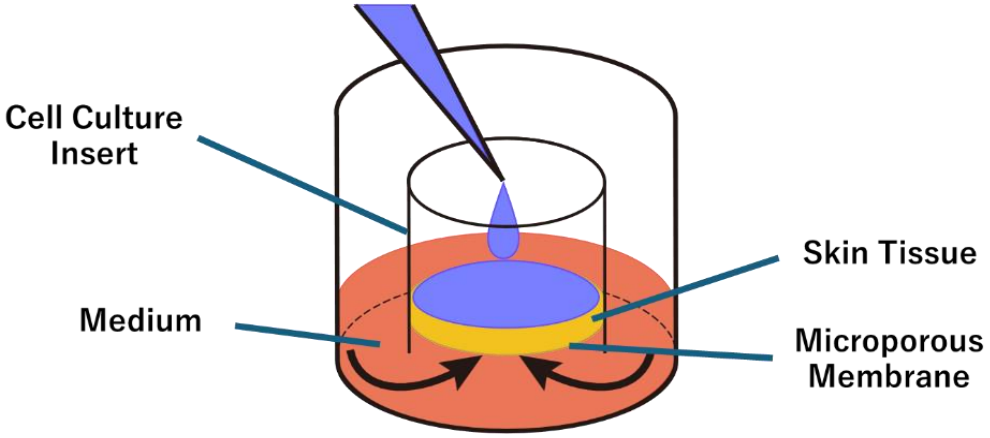

Fig. 1 Structure of the 3D skin model and culture chamber system. Schematic illustration of the multilayered structure of a reconstructed 3D skin model.

CELL CULTURE

The human monocyte line U937 cells (provided by Dr. Keita Takanashi, Yokohama University of Pharmacy) were differentiated into macrophage-like cells. U937 cells were cultured in RPMI-1640 medium containing L-glutamine and phenol red (Fujifilm Wako Pure Chemical Corporation, Osaka, Japan), supplemented with 10% fetal bovine serum (Moregate Biotech, Queensland, Australia), penicillin (100 U/mL), and streptomycin (100 µg/mL) at 37°C in 5% CO_2, and 95% humidified air. Differentiation into macrophage-like cells was induced by treatment with 25 ng/mL phorbol 12-myristate 13-acetate (PMA; Sigma-Aldrich, St. Louis, MO, USA) for 72 h, followed by 48 h incubation in PMA-free medium to promote cell adherence. The procedures followed previously published methods.[20,21]

PREPARATION OF MESENCHYMAL STEM CELL-DERIVED EXOSOMES

Mesenchymal stem cells (MSCs) were purchased from PromoCell (Heidelberg, Germany). Cells were seeded at 5 mL in a T25 flask at a density of 5 x 10^4 cells/mL and cultured in serum-free opti-MEM (Thermo Fisher Scientific, Waltham, MA, USA). After 18 h of culture, the culture supernatants were subjected to the miRCURY exosome isolation kit (product#: 300102; Exiqon, Hovedstaden, Denmark), and purified exosomes were used.

EXPERIMENTS USING THE HUMAN SKIN 3D MODEL

Two 12-well plates (24 chambers in total) were divided into eight groups (n = 3 per group): (1) Control (water), (2) 1% kojic acid (positive control), (3) VB1, (4) VB2, (5) VB3, (6) VB2+VB3, (7) VB2+VB3+MSCs-exosomes, (8) VB1+VB2+VB3. Test materials (100 µL) were applied to the epidermal surface every other day for 3 w. The culture medium in the lower chamber was replaced simultaneously. Images of the skin surface were acquired on days 16 and 22 to monitor the color changes. On day 22, a portion of the skin tissue was fixed in 10% neutral-buffered formalin (Muto Kagaku Co., Tokyo, Japan) for histopathological specimen preparation. Tissue specimens were stained with Hematoxylin and Eosin (H&E) to assess tissue damage and with the Fontana–Masson stain (FM) to detect melanin. The remaining tissue was used for melanin extraction and tyrosinase activity assays. Culture medium from the lower chamber was collected for elemental analysis of metal components in VBs to evaluate their skin permeability.

MEASUREMENT OF MELANIN CONTENT

Melanin content was measured according to the method of Seo et al.[22] On day 22, skin tissue was treated with radio-immunoprecipitation assay (RIPA) buffer to remove proteins, and the residual pellet was incubated with 1 M NaOH at 80 °C for 30 min. Absorbance was measured at 405 nm using the microplate reader and melanin content was calculated from a calibration curve prepared using synthetic melanin (MP Biomedicals, Santa Ana, CA, USA).

TYROSINASE ACTIVITY ASSAY

The tyrosinase activity assay was conducted according to the method described by Di Petrillo et al.[23] Skin tissue harvested on day 22 of culture was solubilized in 0.1 M phosphate buffer (pH 6.8) containing 0.1% Nonidet P-40, and proteins were extracted and quantified using a bicinchoninic acid (BCA) protein assay kit (Takara Bio Inc., Shiga, Japan). Samples were mixed with 2.5 x 10^3 U/mL tyrosinase from mushrooms (Sigma-Aldrich, St. Louis, MO, USA) in 0.1 M phosphate buffer (pH 6.8) and incubated for 15 min at room temperature. Next, 10 mM 3-(3,4-Dihydroxyphenyl)-L-alanine (L-DOPA; Tokyo Chemical Industry Co., Ltd., Tokyo, Japan) was added and incubated at room temperature for 15 min. The absorbance at 475 nm was then measured using a microplate reader to quantify the generated dopaquinone.

DETECTION OF METAL ELEMENTS CONTAINED IN VBS FOR VERIFYING SKIN PERMEABILITY

The metal elements contained in the VBs (W: tungsten, Sb: antimony, V: vanadium, and S: sulfur) were quantified using an energy-dispersive X-ray fluorescence analyzer (EDX-7000, SHIMADZU, Kyoto). For the purpose of evaluating skin permeability, the amount of metal elements in the 100 µl of liquid applied to the epidermis was designated as 100%. Skin permeability was quantified as the percentage of each metal element that permeated through the skin tissue and accumulated in the culture medium of the lower chamber.

MODULATORY EFFECTS OF VBS ON MACROPHAGE ACTIVITY

mRNA expression. Total RNA was extracted using TRIzol reagent (Ambion, Austin, TX, USA) according to the manufacturer's instructions. The mRNA expression levels of inducible nitric oxide synthase (iNOS), STAB1[24], and FGF2[25] were determined using one-step quantitative reverse transcription polymerase chain reaction (qRT-PCR) with specific primers (Table 1). Specifically, a one-step PCR was performed in the same tube using the Luna Universal One-Step qRT-PCR Kit (New England Biolabs, Ipswich, MA, USA) and Thermal Cycler Dice Real Time System II (Takara Bio, Shiga, Japan). Reactions were performed according to the manufacturer's instructions for the reagent kit. Delta Ct was calculated with an internal standard using the constantly expressed gene, glyceraldehyde-3-phosphate dehydrogenase (GAPDH).[26] Differences from experimental controls were determined using the delta-delta Ct method[27] and expressed as fold changes in mRNA expression.

NO production. Nitrite in the culture supernatant was measured colorimetrically using the Nitrate/

Nitrite Colorimetric Assay Kit (Cayman Chemical, Ann Arbor, MI, USA). Lipopolysaccharide (LPS; 0.1 or 1 µg/mL; Macrophi Inc., Kagawa, Japan) was used as a positive control.

Phagocytic capacity. To assess phagocytic activity, macrophages were co-incubated with fluorescent latex beads and VBs for 24 h. Subsequently, cells were washed with phosphate-buffered saline (PBS) to eliminate free-floating beads. The beads phagocytosed by macrophages were visualized using a fluorescence microscope (BZ-X710, Keyence, Osaka, Japan). Phagocytic activity was quantified by comparing the fluorescence intensity of each experimental group to that of the untreated control, which was defined as 100%. LPS (0.1 or 1 µg/mL) was used as a positive control.[28]

Table 1 Specific primers used for the detection of mRNA expression of iNOS, STAB1, and FGF2 with one-step quantitative reverse transcription polymerase chain reaction

Gene	Primer	References
iNOS	Forward: GGACATCACCACACCCCCAACAC	R&D system Cat# RDP-101
	Reverse: GCCCTTCCGCAGTTTCTGGCAGCA	
STAB1	Forward: GAACCATGTGCCACTGGAAGGC	[24]
	Reverse: AGCGGAATCTCCTGGTGCAGTT	
FGF2	Forward: ACTTGGAGGCTTATCTACCTGT	[25]
	Reverse: CCAGCATTTCGGTGTTGAAGA	
GAPDH	Forward: GACATGCCGCCTGGAGAAAC	[26]
	Reverse: AGCCCAGGATGCCCTTTAGT	

Results

ANALYSIS OF EPIDERMAL IMAGES USING A 3D SKIN MODEL

Skin surface images were captured on days 16 and 22 following the repeated application of each sample to the epidermal surface (Fig. 2). In all groups, pigmentation appeared to progress between days 16 and 22. The group treated with 1% kojic acid exhibited a visibly lighter color compared to the control group on both observation days, whereas no clear visual changes were observed in any of the VB-treated groups. The acquired images were converted to grayscale (0–255) for quantitative analysis (Fig. 2). Quantification confirmed that only the kojic acid group exhibited a marked decrease in pigmentation relative to the control on both days 16 and 22, whereas no marked differences were detected in the other groups.

HISTOLOGICAL ANALYSIS OF THE 3D SKIN MODEL

On day 22, skin tissues were fixed in 10% neutral buffered formalin, sectioned, and subjected to H&E and FM stains (Fig. 3a). Hematoxylin and Eosin staining showed that the nuclei remained intact, but the 1% kojic acid group exhibited alterations in epidermal architecture, such as loss of the spinous layer and thinning of the stratum corneum. Although the VB1 group generally exhibited weak staining, the VB2 group maintained a distinct layered structure with pronounced thickening and folding of the spinous layer. Image analysis of melanin-positive regions visualized using FM staining demonstrated a marked reduction in melanin content in the 1% kojic acid group (Fig. 3b). A comparable reduction in melanin synthesis was observed in the VB2 single-treatment group and the combination treatment group with VB1, VB2 and VB3.

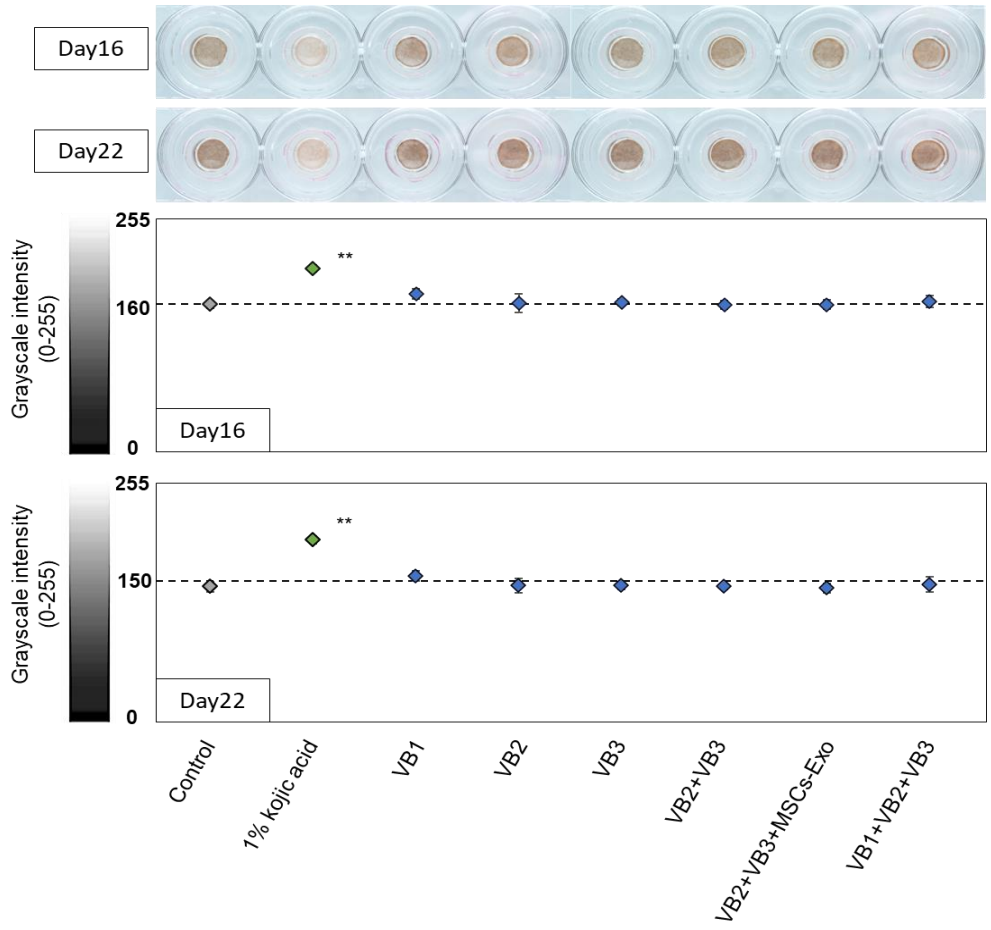

Fig. 2 Evaluation of pigmentation in 3D skin model. Representative images of 3D skin model plates at 16 and 22 days of culture. Grayscale conversion (0–255) was applied to the images, and pigmentation intensity was quantified based on grayscale values. Data are expressed as mean ± SD (n = 3). The statistical significance is indicated as $^{**}p < 0.01$ vs. control

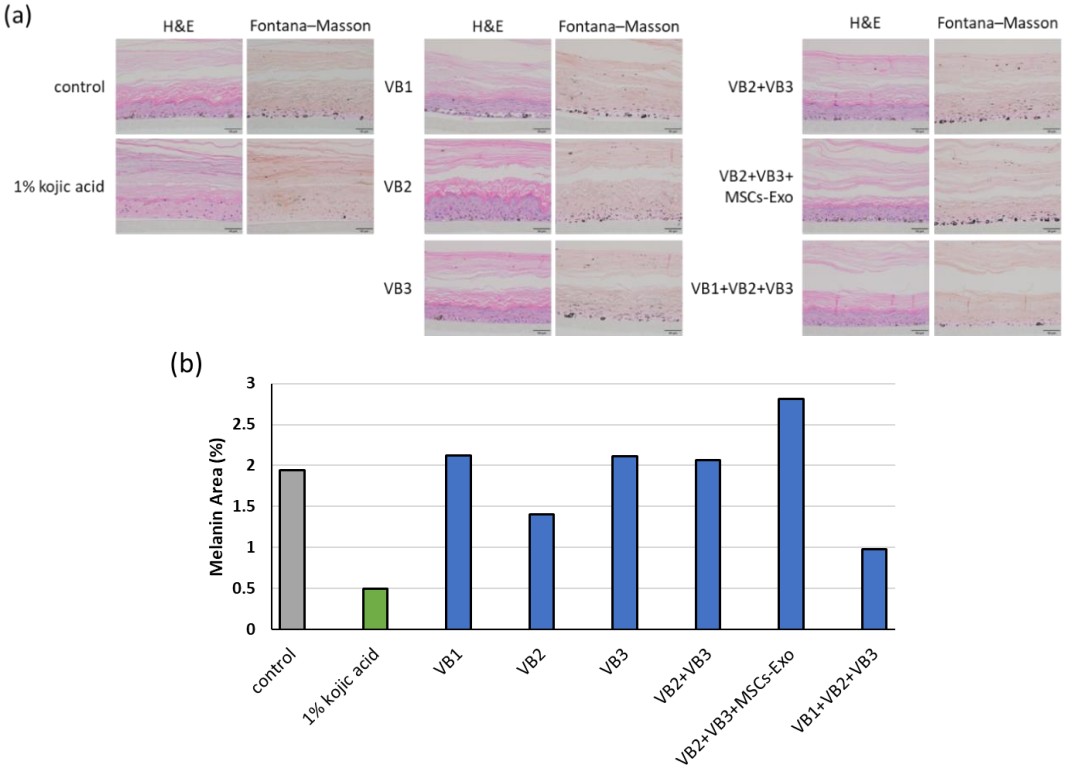

Fig. 3 Histological staining of the 3D skin model and quantitative analysis of melanin content. (a) H&E and FM stains of the skin tissue sections obtained on day 22. (b) Image analysis of melanin-positive regions visualized using FM staining.

MEASUREMENT OF MELANIN AND TYROSINASE ACTIVITY IN THE 3D SKIN MODEL

Melanin content and tyrosinase activity were measured in tissues collected from diffusion chambers. Melanin content was markedly reduced in the 1% kojic acid group, as well as in groups treated with VB1, VB2, and VB3 individually, and in combination (Fig. 4a). Among the groups treated with VBs, VB2 alone exhibited the strongest inhibitory effect on melanin production. Although no statistically significant differences in tyrosinase activity were observed among the groups, both the VB2 group and the VB1+VB2+VB3 combination group—both of which showed lower melanin levels—tended to suppress tyrosinase activity to a degree comparable to those of 1% kojic acid (Fig. 4b).

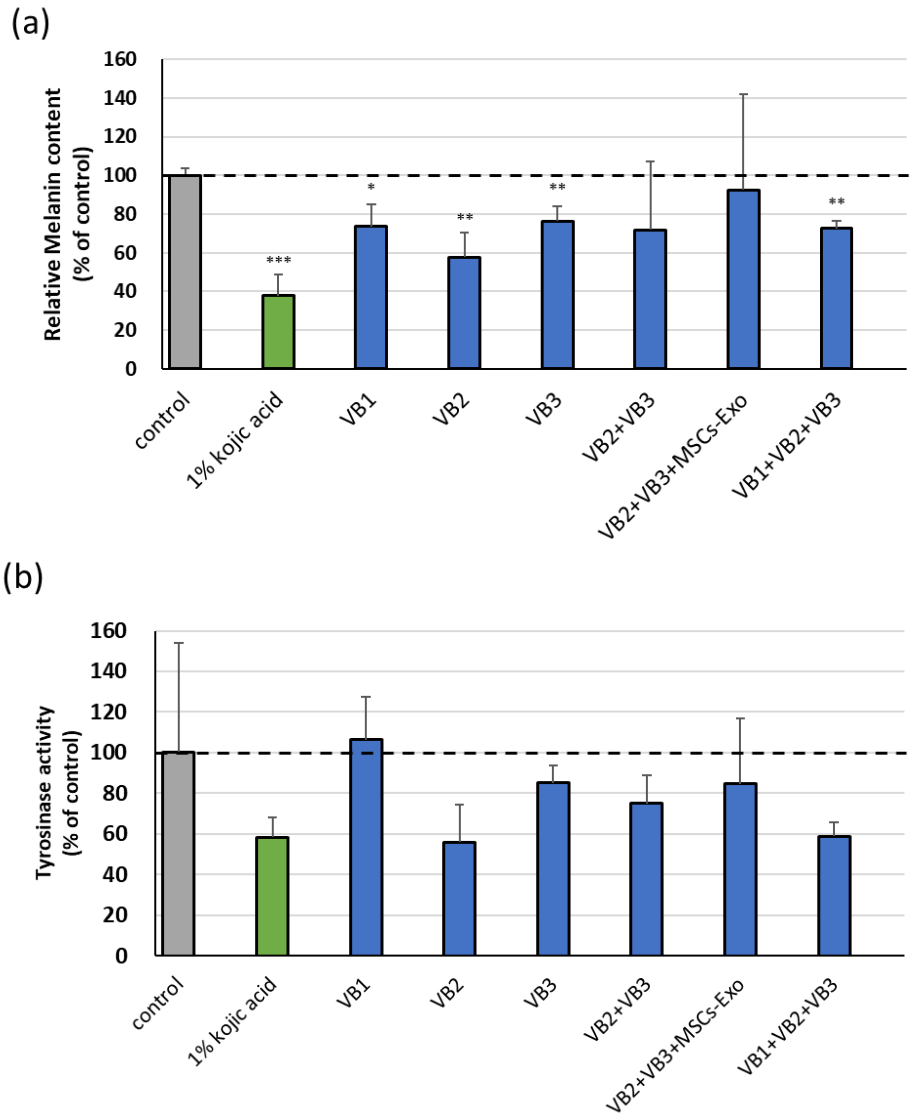

Fig. 4 Measurement of melanin content and tyrosinase activity in the 3D skin model
(a) Melanin content in skin tissue measured on day 22. (b) Tyrosinase activity was measured using a colorimetric assay. Protein extracts were prepared from skin tissue collected on day 22. Data: mean ± SD (n = 3). *p <0.05, **p <0.01, ***p <0.001 vs. control

DETECTION OF CONSTITUENT ELEMENTS FOR EVALUATING SKIN PERMEABILITY OF VBS

Skin permeability was assessed by quantifying the elemental components (V, S, W, and Sb) of the VBs in the culture medium collected from the lower chamber. In all the VB-treated groups, the presence of these elements was detected as early as 1 h after reagent application (Fig. 5a). No marked change in their concentrations was observed after 24 or 48 h, suggesting that the permeation process had reached a steady state. The highest permeability at 24 h was observed in the VB1 alone group (49.6%), followed by the VB1, VB2, and VB3 combination groups (33.3%) (Fig. 5b).

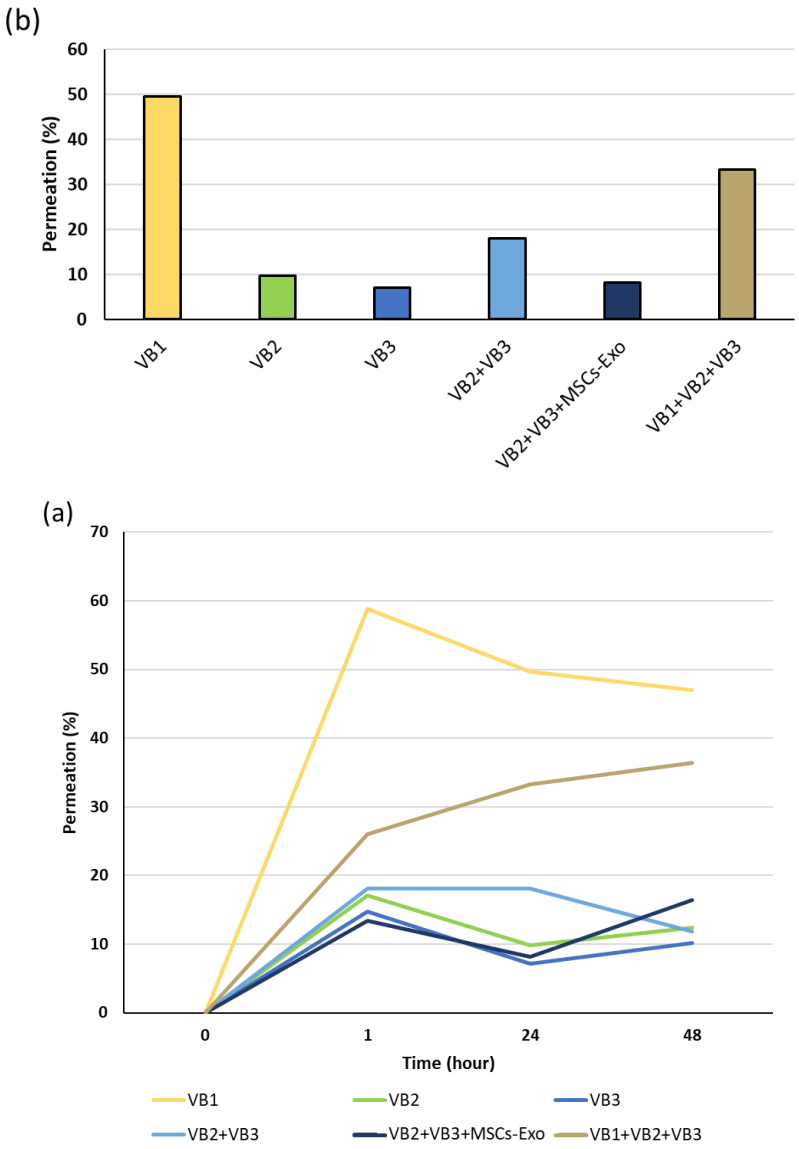

Fig. 5 Evaluation of skin permeability of VBs in the 3D skin model
The amount of VBs that penetrated the lower chamber was quantified by detecting VB constituent elements. (a) Time course of VB permeability at 1, 24, and 48 h. (b) Permeation of VBs measured at 24 h of culture.

REGULATORY EFFECTS OF VBS ON MACROPHAGE FUNCTION

Since VBs were found to permeate the epidermis, they may also affect macrophage function in the dermis. Therefore, we conducted an analysis of the effects of VBs on macrophage activity (Fig. 6). Quantitative reverse transcription polymerase chain reaction analysis showed slight increases in iNOS expression, with a statistically significant elevation in the VB3 group (delta-delta Ct ≥2). Stabilin-1 (STAB1), a molecule that recognizes senescent cells, exhibited an increasing trend in VB1 and VB3 groups. Fibroblast growth factor-2 (FGF2), a factor that promotes regenerative signaling to nearby stem cells following macrophage phagocytosis, also exhibited an increase, especially in the VB1 and VB3 groups.

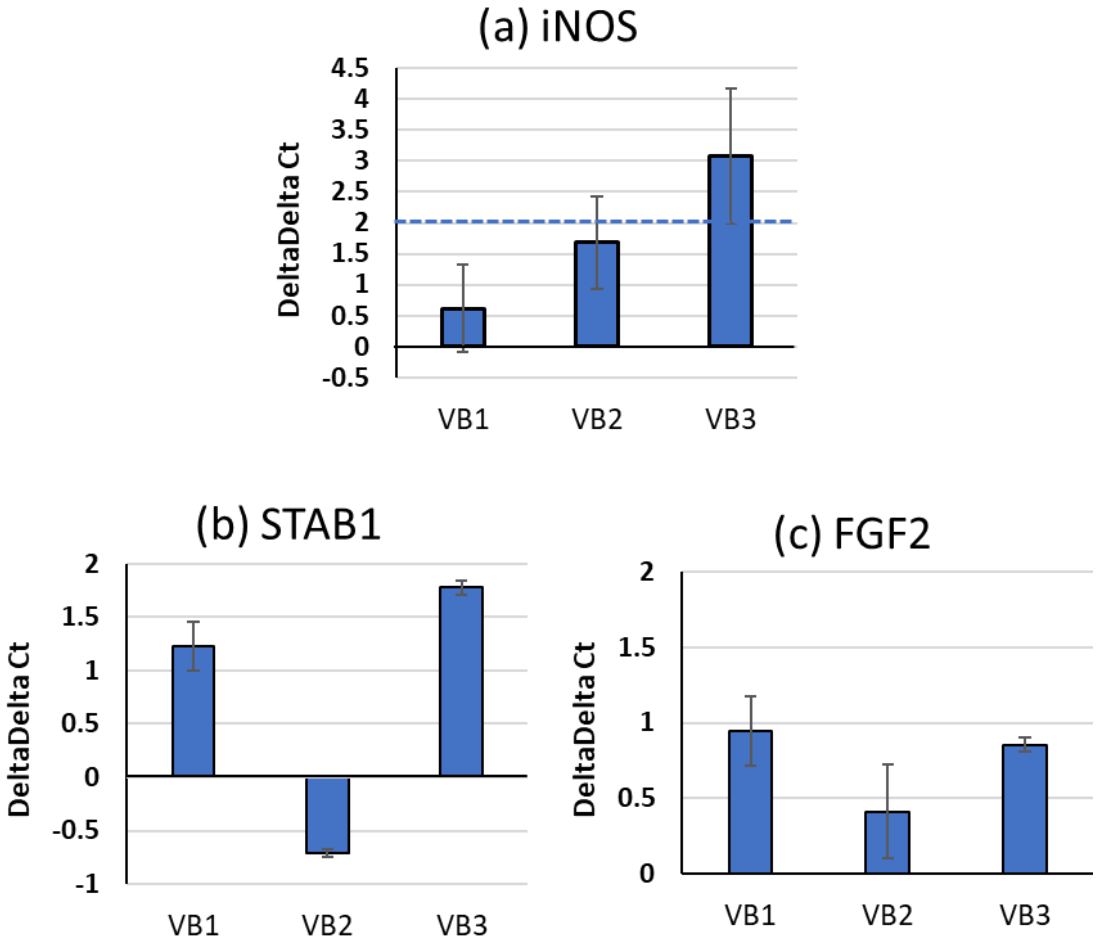

Fig. 6 Analysis of macrophage activation using quantitative real-time polymerase chain reaction (PCR) The mRNA expression levels of iNOS (a), STAB1 (b), FGF2 (c) were quantified in macrophages treated with VBs. A significant difference is evident when the delta-delta Ct value differs by more than two-fold over the control.

Because VB3 markedly increased iNOS mRNA expression, the nitrite levels produced by the macrophages were quantified (Fig. 7). Lipopolysaccharide, used as a positive control, elicited a dose-dependent response, with stimulation at 1 µg/mL resulting in significantly enhanced NO production (Fig. 7). Nitrite production was markedly increased upon stimulation with all groups except VB1. The degree of increase corresponded well with the tendencies observed in the iNOS mRNA levels. Treatment with VB3 alone exhibited the strongest effect, whereas an additive effect was not observed when VB2 and VB3 were combined.

Phagocytic activity of macrophages was subsequently evaluated using fluorescent bead uptake (Fig. 8). Representative fluorescent images (upper panel) indicate that phagocytic activity was increased upon stimulation with 0.1 and 1 µg/mL LPS. The relative fluorescence intensity of each group (lower panel) was calculated using the control set as 100%. Using this system, VB treatment substantially enhanced the phagocytic activity in all groups. Notably, VB3 exhibited strong activity, which remained unaffected by co-treatment with either VB2 or VB1.

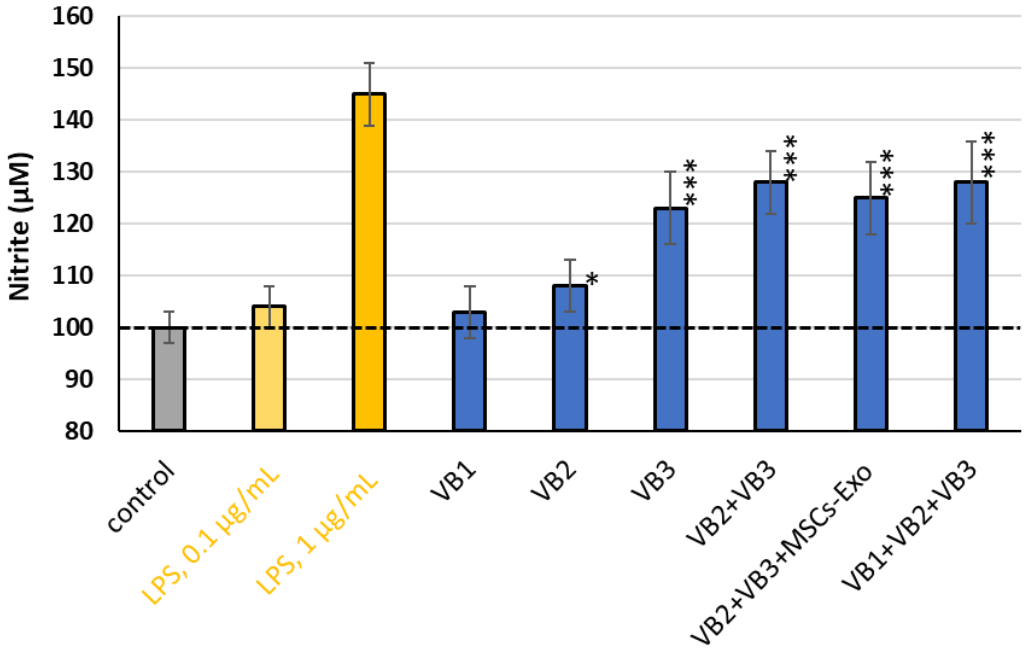

Fig. 7 Measurement of NO production in macrophages
Nitrite in the culture supernatants were measured using the Nitrate/Nitrite Colorimetric assay kit. The statistical significance is indicated as* p <0.05, *** p <0.001 vs. control

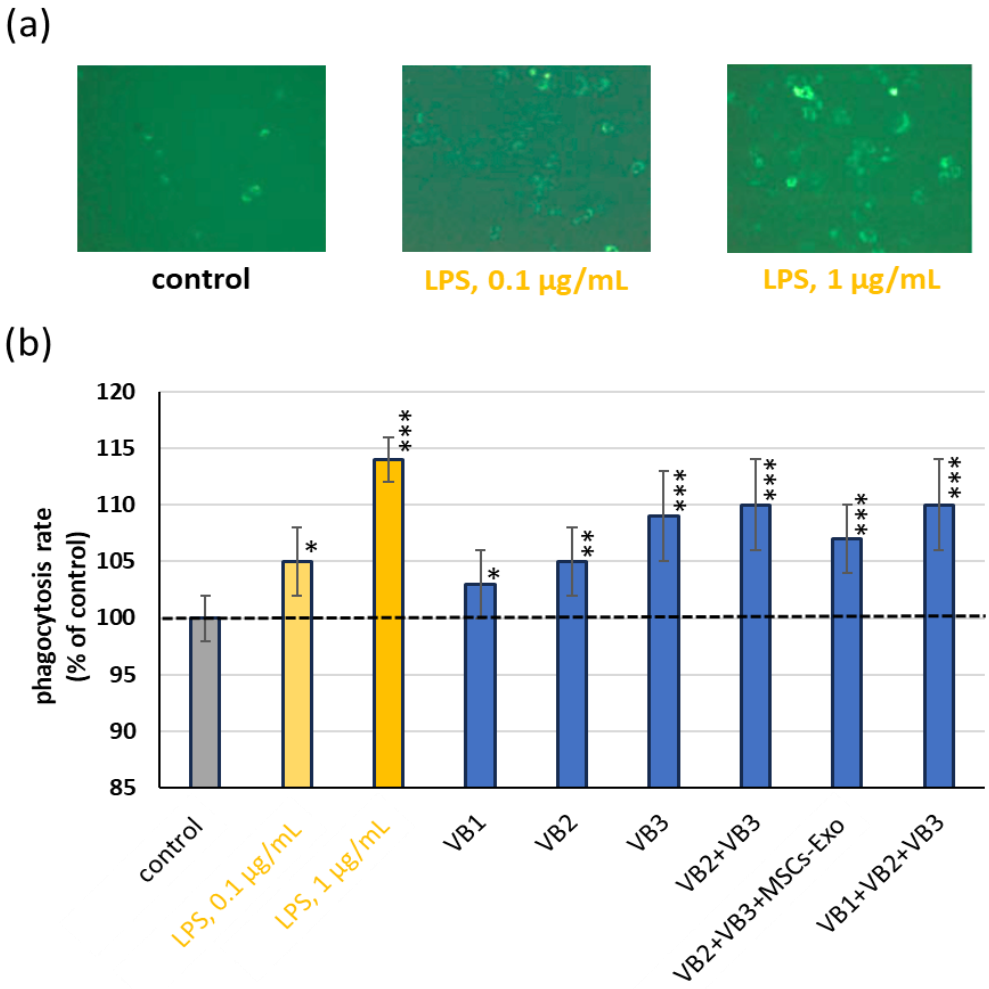

Fig. 8 Evaluation of phagocytic activity in macrophages using latex beads
(a) Representative fluorescence images of macrophages after stimulation with or without LPS (0.1 and 1 μg/mL). (b) Quantitative analysis of phagocytic activity based on the fluorescence intensity after incubation with latex beads. * p <0.05, ** p <0.01, *** p <0.001 vs. control

Discussion

Based on their previously reported antibacterial and antiviral activities, VB1, VB2, and VB3, which were selected from polyoxometalates (PM), were evaluated for potential application to the skin. These compounds were previously shown to reduce ROS accumulation in fibroblasts subjected to oxidative stress induced by hydrogen peroxide.[16] In this study, skin permeability and the effects of repeated VB treatment on melanin synthesis were evaluated using the 3D skin model, which more closely mimics the *in vivo* skin environment than conventional monolayer cultures. An additional analysis was conducted to investigate the potential effects of VBs on macrophages, as part of a broader assessment of their impact on the dermal layer.

Hematoxylin and Eosin staining indicated structural alterations and thinning of the stratum corneum in the 1% kojic acid group (Fig. 3a), suggesting suppression of keratinocyte proliferation and differentiation. Kojic acid is widely used as a skin-whitening ingredient in cosmetics and quasi-drugs in Japan. According to the Cosmetics Ingredient Review (CIR), kojic acid is considered safe for use in cosmetics at concentrations below 1%.[29] The present study used a reconstructed skin tissue model composed of both melanocytes and keratinocytes, suggesting that the observed effects may be more pronounced than in actual human application. Given that 1% kojic acid exhibited mild cytotoxicity, a lower concentration might have been more appropriate for this experiment.[19]

Following stimulation with VBs, mild suppression of differentiation was observed in the VB1-alone group, various VB combination groups, and the VB—exosome combination group, suggesting a potential reduction in cellular activity. In contrast, VB2- and VB3-alone preserved or enhanced epidermal architecture, indicating the promotion of active keratinocyte differentiation.

The cells used in this 3D skin model were derived from individuals of African descent and can be maintained in culture for approximately 3 w. The control gradually darkened and reached a stable tone after approximately 2 w (Fig. 2). The positive control, 1% kojic acid, which is a tyrosinase inhibitor, showed a consistent and sustained inhibitory effect. In contrast, the VB-treated groups showed no obvious suppression of pigmentation either visually or using the grayscale image analysis (Fig. 2). However, A more detailed analysis using the histological specimens by FM staining indicated a reduction in melanin in the VB2 single-treatment group and in the combination of VB1, VB2, and VB3 (Fig. 3).

To more thoroughly examine the effects of VBs on melanin synthesis, melanin was extracted and quantified, and tyrosinase activity in the skin tissue was measured on day 22 (Fig. 4a, b). When Compared with the control group, marked reductions in melanin content were observed in all single-treatment groups (VB1, VB2, and VB3) throughout the skin tissue in the chamber, with VB2 showing the strongest inhibitory effect. When VB2 was combined with VB3 or VB1, the values tended to return toward the mean. This suggests that these combinations did not enhance the inhibitory effect beyond that of VB2 alone. In addition, the combination of VB2 and VB3 with stem cell-derived exosomes did not further enhance the inhibitory effect. This finding alone does not rule out the involvement of exosomes in melanin synthesis, and further investigation is warranted.

Although no statistically significant difference was observed in tyrosinase activity, likely due to the high variability in the control group, melanin content was correlated with tyrosinase activity. Tyrosinase catalyzes the initial steps of melanin biosynthesis, converting tyrosine to L-DOPA and subsequently to dopaquinone, and the observed reduction suggest that VBs may specifically inhibit this early stage of the pathway.[30] On the other hand, according to previous studies, kojic acid inhibits tyrosinase by chelating copper ions and also suppress the maturation of melanosomes and their transfer to keratinocytes, indicating that kojic acid inhibits not only tyrosinase activity but also the subsequent

process of melanin accumulation, thereby markedly suppressing skin pigmentation.[31] Further detailed investigation is required to determine whether the suppression of pigmentation by VBs results solely from the inhibition of tyrosinase activity, or if it also involves interference with melanosome maturation or melanosome–keratinocyte transfer.

VBs have been reported to enhance cysteine uptake in human skin fibroblasts, thereby promoting the elimination of ROS.[17] In particular, VB2 has been shown to strongly enhance the uptake of cystine. In the melanin biosynthesis pathway, the reaction of cysteine with dopaquinone redirects melanin production from black melanin (eumelanin) to yellow melanin (pheomelanin).[10] In the current study, FM staining indicated that all VBs markedly inhibited melanin production. In particular, VB2 exhibited a strong inhibitory effect on melanin synthesis. While the precise mechanism remains unclear, it is plausible that the suppression of total melanin content may result from a metabolic shift from the eumelanin to the pheomelanin pathway, possibly through activation of the cysteine-dependent branch. Future studies will focus on analyzing the effects of VBs on cystine uptake in melanocytes, with the goal of elucidating the comprehensive mechanism underlying VB-mediated suppression of melanin synthesis.

The penetration of VBs added to the skin surface into the epidermis and its subsequent passage into the dermis was evaluated by detecting the VB-associated elements in the culture medium. All VBs were detected in the lower chamber within 1 h of their addition, indicating that they exhibit epidermal permeability. The penetration rate was the highest for VB1 (approximately 60%), whereas VB2 and VB3 showed rates below 20% (Fig. 5). This difference is likely attributable to the molecular weight of each compound. The approximate molecular weights were: VB1, 79 Da; VB2, 2,535 Da; and VB3, 1,201 Da. Therefore, the high permeability of VB1 is consistent with its smaller molecular weight. In general, molecules with a molecular weight below ~500 Da are considered capable of penetrating the skin barrier.[32] VB2 and VB3, whose molecular weights far exceeded this threshold, still permeated to nearly 20%. Although the molecular weight of VB2 was approximately twice that of VB3, the permeation rates were comparable. This may be influenced by factors such as differences in molecular polarity, or charge distribution. In addition, the involvement of mechanisms other than passive diffusion on the epidermal side cannot be excluded. For example, the behavior of VBs after cellular entry may be regulated by active transport processes mediated by transporters expressed in the epidermis. ATP-binding cassette (ABC) transporters expressed in the skin are known to regulate the efflux and intracellular distribution of compounds using adenosine triphosphate (ATP), and these transporters may influence intracellular retention and efflux directionality of VBs, thereby contributing to the final permeation amount and the extent of delivery to the dermal compartment.[33] However, the precise mechanism remains unclear. Notably, all VBs permeated rapidly and showed consistent permeation rates even after repeated application, and no cytotoxic effects were observed. Further pharmacokinetic investigations are required to determine the retention time of VB within the epidermis after a single application, and to clarify the extent and kinetics of its long-term permeation.

Since it was found that VBs can permeate through the epidermis, we investigated whether VBs influenced macrophage activity (Figs 6–8). VB3 markedly increased iNOS mRNA expression, an indicator of macrophage activation, whereas VB1 and VB2 showed less pronounced increases. Nitrite production was consistently elevated in groups treated with VB2, and VB3. Macrophages are broadly classified into inflammatory macrophages (M1) and macrophages involved in tissue repair and regeneration (M2), based on their functional properties.[34] In this study, VB3 treatment markedly increased the expression of iNOS, a commonly used marker of inflammatory (M1-like) macrophage activation.[35] This result suggests that VBs may promote M1-like inflammatory responses in macrophages.

A mechanism has been identified in skin tissue in which macrophages recognize and phagocytose senescent cells, subsequently sending signals to surrounding skin stem cells to promote regeneration. The molecules involved in this process include STAB1, which facilitates the recognition and clearance of senescent cells, and FGF2, which promotes the activation of skin stem cells following their phagocytosis.[13] VB1 and VB3 appeared to upregulate the mRNA levels of these molecules. Furthermore, assessment of phagocytic activity using fluorescent beads revealed that VB3 showed the highest activity, followed by VB2 and VB1. These results suggest that VBs not only enhance the inflammatory response of macrophages but may also stimulate their regenerative signaling pathways. Specifically, when senescent cells emerge in the dermis, VBs may facilitate macrophage-mediated recognition and clearance, while concurrently promoting the regeneration of adjacent skin stem cells. Further detailed studies examining the concentration dependence of VBs and their time-course effects are warranted to more precisely elucidate the underlying mechanisms.

Conclusions

Using the 3D skin model, VBs inhibited melanin synthesis by blocking tyrosinase activity. It is likely that VBs that penetrate the dermis are able to activate macrophages located in the skin. This activation may influence the expression of STAB1, an adhesion molecule involved in the recognition of senescent cells. It may also affect FGF2, a growth factor that promotes regeneration. These findings suggest that VBs participate in both pigmentation control and novel mechanisms of skin regeneration.

As the effects on melanin synthesis varied slightly among VB1, VB2, and VB3, their combined use may enhance efficacy by producing additive or synergistic effects. These VBs exhibited no cytotoxicity even after repeated skin applications, indicating their potential as safe cosmetic ingredients with dual functions, namely regulation of skin pigmentation and activation of dermal immune responses.

Conflicts of Interest:

The authors have no conflicts of interest to declare.

Funding Statement:

This study received no external funding.

Acknowledgments:

We express our sincere gratitude to Dr. Keita Takanashi (Yokohama Pharmaceutical University) for providing the human monocytic U937 cell line. We also extend our gratitude to FSX Company and to all individuals involved in the development of VB-compounded hygienic products for their generous cooperation.

References:

1. Dainichi T, Kitoh A, Otsuka A, Nakajima S, Nomura T, Kaplan DH, Kabashima K. The epithelial immune microenvironment (EIME) in atopic dermatitis and psoriasis. *Nat Immunol*. 2018;19(12):1286–1298

2. Kabashima K, Honda T, Ginhoux F, Egawa G. The immunological anatomy of the skin. *Nat Rev Immunol*. 2019;19(1):19–30.

3. Brunet A, Goodell MA, Rando TA. Ageing and rejuvenation of tissue stem cells and their niches. *Nat Rev Mol Cell Biol*. 2023;24(1):45–62.

4. Fujimoto A, Iwai Y, Ishikawa T, Shinkuma S, Shido K, Yamasaki K, Fujisawa Y, Fujimoto M, Muramatsu S, Abe R. Deep neural network for early image diagnosis of Stevens–Johnson syndrome/toxic epidermal necrolysis. *J Allergy Clin Immunol Pract.* 2022;10(1):277–283.

5. Matsui T, Amagai M. Dissecting the formation, structure, and barrier function of the stratum corneum. *Int Immunol*. 2015;27(6):269–280.

6. Proksch E, Brandner JM, Jensen JM. The skin: An indispensable barrier. *Exp Dermatol*. 2008;17 (12):1063–1072.

7. Tracy LE, Minasian RA, Caterson EJ. Extracellular matrix and dermal fibroblast function in the healing wound. *Adv Wound Care* (New Rochelle). 2016;5 (3):119–136.

8. Yamashita T, Kuwahara T, González S, Takahashi M. Non-invasive visualization of melanin and melanocytes by reflectance-mode confocal microscopy. *J Invest Dermatol*. 2005;124(1):235–240.

9. Yoshikawa-Murakami C, Mizutani Y, Ryu A, Naru E, Teramura T, Homma Y, Fukuda M. A novel method for visualizing melanosome and melanin distribution in human skin tissues. *Int J Mol Sci*. 2020;21(22):8514.

10. Boo YC. Metabolic basis and clinical evidence for skin lightening effects of thiol compounds. *Antioxidants* (Basel). 2022;11(3):503.

11. Kupper TS, Fuhlbrigge RC. Immune surveillance in the skin: Mechanisms and clinical consequences. *Nat Rev Immunol*. 2004;4(3):211–222.

12. Muñoz J, Akhavan NS, Mullins AP, Arjmandi BH. Macrophage polarization and osteoporosis: A review. *Nutrients*. 2020;12(10):2999.

13. Ogata Y, Yamada T, Hasegawa S, Sugiura K, Akamatsu H. Changes of senescent cell accumulation and removal in skin tissue with ageing. *Exp Dermatol.* 2023;32(7):1159–1161.

14. Dan K, Yeh H-L. Biological activity of polyoxometalates and their applications in anti-aging. *Med Res Arch.* 2024;12(12).

15. Dan K, Fujinami K, Sumitomo H, Ogiwara Y, Suhara S, Konno Y, Sawada M, Soga Y, Takada A, Takanashi K, Watanabe K, Shinozuka T. Application of antiviral polyoxometalates to living environments: Antiviral moist hand towels and stationery items. *Appl Sci.* 2020;10:8246

16. Fujinami K, Dan K, Tanaka-Kagawa T, Kawamura I. Anti-aging effects of polyoxometalates on skin. *Appl Sci.* 2021;11(24):11948.

17. Fujinami K, Dan K, Tominaga N, Tanaka-Kagawa T, Kawamura I. Enhancing effect of polyoxometalates on the aging stress responses of skin cells. *Med Res Arch.* 2025;13(8).

18. Bessou-Touya S, Picardo M, Maresca V, Surleve-Bazeille JE, Pain C, Taieb A. Chimeric human epidermal reconstructs to study the role of melanocytes and keratinocytes in pigmentation and photoprotection. *J Invest Dermatol.* 1998;111: 1103–1108.

19. Zöller NN, Hofmann M, Butting M, Hrgovic I, Bereiter-Hahn J, Bernd A, Kaufmann R, Kippenberger S, Valesky E. Assessment of Melanogenesis in a pigmented human tissue-cultured skin equivalent. *Indian J Dermatol*. 2019;64(2):85–89.

20. Sumiya Y, Ishikawa M, Inoue T, Inui T, Kuchiike D, Kubo K, Uto Y, et al. Macrophage activation mechanisms in human monocytic cell line-derived macrophages. *Anticancer Res.* 2015;35:4447–4451.

21. Xie C, Liu C, Wu B, Lin Y, Ma T, Xiong H, Wang Q, et al. Effects of IRF1 and IFN-β interaction on the M1 polarization of macrophages and its antitumor function. *Int J Mol Med.* 2016;38:148–160.

22. Seo G-Y, Ha Y, Park A-H, Kwon OW, Kim Y-J. *Leathesia difformis* extract inhibits α-MSH-induced melanogenesis in B16F10 cells via down-regulation of CREB signaling pathway. *Int J Mol Sci*. 2019;20: 536.

23. Di Petrillo A, González-Paramás AM, Era B, et al. Tyrosinase inhibition and antioxidant properties of *Asphodelus microcarpus* extracts. *BMC Complement Altern Med.* 2016;16:453.

24. Shay JW, Homma N, Zhou R, Naseer MI, Chaudhary AG, Al-Qahtani M, et al. Abstracts from the 3rd International Genomic Medicine Conference (3rd IGMC 2015). Jeddah, Kingdom of Saudi Arabia. 30 November–3 December 2015. *BMC Genomics*. 2016;17(Suppl 6):487.

25. Kok SY, Oshima H, Takahashi K, Nakayama M, Murakami K, Ueda HR, Miyazono K, Oshima M. Malignant subclone drives metastasis of genetically and phenotypically heterogenous cell clusters through fibrotic niche generation. *Nat Commun*. 2021;12 (1):863.

26. Liu W, Ma C, Li H-Y, Chen L, Yuan S-S, Li K-J. MicroRNA-146a downregulates the production of hyaluronic acid and collagen I in Graves' ophthalmopathy orbital fibroblasts. *Exp Ther Med*. 2020;20(5):38.

27. Rao, X., Huang, X., Zhou, Z., Lin, X. (2013). An improvement of the 2ˆ(-delta-delta CT) method for quantitative real-time polymerase chain reaction data analysis. Biostat Bioinforma Biomath, 3 (3),71-85.

28. Haron MH, Tyler HL, Pugh ND, Jackson CR, Pasco DS. *In vitro* macrophage activation by edible mushroom extracts varies considerably and is highly correlated to bacterial LPS content. *PlantaMed.* 2014;80:12.

29. Burnett CL, Bergfeld WF, Belsito DV, Hill RA, Klaassen CD, Liebler DC, Marks JG Jr, Shank RC, Slaga TJ, Snyder PW, Andersen FA. Final report of the safety assessment of Kojic acid as used in cosmetics. *Int J Toxicol*. 2010;29(Suppl 6):244S-73.

30. Slominski A, Zmijewski MA, Pawelek J. L-tyrosine and L-dihydroxyphenylalanine as hormone-like regulators of melanocyte functions. *Pigment Cell Melanoma Res*. 2012;25(1):14–27.

31. Cardoso R, Valente R, Souza da Costa CH, da S. Gonçalves Vianez JL Jr., Santana da Costa K, de Molfetta FA, Nahum Alves C. Analysis of kojic acid derivatives as competitive inhibitors of tyrosinase: A molecular modeling approach. Molecules. 2021; 26(10):2875.

32. Bos JD, Meinardi MM. The 500 Dalton rule for the skin penetration of chemical compounds and drugs. *Exp Dermatol*. 2000;9(3):165–169.

33. Nielsen MMK, Aryal E, Safari E, Mojsoska B, Jenssen H, Prabhala BK. Current State of SLC and ABC Transporters in the Skin and Their Relation to Sweat Metabolites and Skin Diseases. *Proteomes*. 2021;9(2):23.

34. Murray PJ, Allen JE, Biswas SK, et al. Macrophage activation and polarization: nomenclature and experimental guidelines. *Immunity*. 2014;41(1):14-20.

35. Martinez FO, Gordon S. The M1 and M2 paradigm of macrophage activation: time for reassessment. *F1000Prime Rep*. 2014;6:13.

